World Journal of Earth and Planetary Sciences
Vol. 1, No. 1, December 2014, pp. 1- 22
Available online at http://wjeps.com/

Research article

Gabal El Faliq granitoid rocks of the southeastern Desert, Egypt: Geochemicalconstraints, mineralization and spectrometric prospecting

Gehad M. Saleh[1], Ibrahim A. Salem[2], Mostafa E. Darwish[1] and Doaa A. Mostafa [1]

1-Nuclear Materials Authority, P. O. Box: 530 El Maadi, Cairo, Egypt.
2-Tanta University, Faculty of Science, Geology Depart. Tanta, Egypt.
E- mail: drgehad_m@ yahoo.com

Abstract

The granitoid rocks in G. El Faliq area, southeastern Desert of Egypt, consist of granodiorites, tonalities, monzogranites and alkali feldspar granites. The G. El-Faliq area is composed of ophiolitic mélange, gneisses, older granitoids, younger granitoids and post granitic dykes and veins. Altered granites are encountered at shears and fault zones enriched with uranium and base metals mineralization. Geochemically, the older granitoids are peraluminous to metaluminous identical to volcanic arc granites, while the younger granitoids are calc-alkaline and metaluminous to peralkaline granites and display chemical characteristics within plates' granite setting. The altered granites show argilic facies with a relative depletion in K_2O and Na_2O + CaO. The comparison between the average compositions of the major oxides of the fresh samples of younger granitoids relative to altered ones in the studied area shows that, the younger granitoids enriched in SiO_2, Na_2O and K_2O but depleted in TiO_2, Al_2O_3, Fe_2O_3, FeO, MnO, CaO, MgO and P_2O_5. Also, with regard to their trace elements content they are enriched in Sr and depleted in Ni, Zn, Zr, Y, Ba, Nb, U and Th. The mineralization of G. El Faliq can be classified on the basis of mode of occurrence and lithological associations into: a) secondary uranium minerals (uranophane), b) niobium-tantalum minerals, c) sulphide minerals and d) accessory minerals. The spectrometric survey revealed the presence of enriched zones with a maximum eU content of 650 ppm and the maximum eTh is 350 ppm. The evidence of hydrothermal mineralization can be seen in the alteration of rock-forming minerals such as feldspars and the formation of secondary minerals such as uranophane and pyrite. The pre-existing primary uranium minerals are the source of the present secondary uranium minerals by the action of oxidizing fluids, mobilization of uranium and then redeposition in other forms. Redistribution by circulating meteoric waters might have taken place.

Key words: G. El-Faliq, uranium mineralization, spectrometric prospecting, granitoids.

1. Introduction

The Precambrian rocks of Egypt represent the western part of the Arabian- Nubian Shield, which was formed during the Pan-African orogenic cycle (950-450 Ma) by the accretion of juvenile arc terranes, followed by crustal thickening accompanied by intrusion of batholiths of predominantly granitic composition[1]. Different classifications of the Egyptian granitoids were based on field relations, tectonic and geochronological determinations ([2], [3],[4],[5],[6],[7],[8],[9] and [10]. Most of the younger granites are (large ionic lithophile

elements) LILE-enriched calc-alkaline to mildly alkaline rocks with I-type affinity, but some of them have been recently classified as A-type [11] and [12]. However, both I-and A-type Egyptian younger granitoids are epizonal plutons emplaced at shallow crustal levels along an active continental margin [13]. Several models are proposed for the origin of the Egyptian younger granites which include the following: 1) Partial melting of lower crust [10], [14], [15] and [16] ; 2) Assimilation of pre- Pan-African old continental crust by mantle-derived mafic melts [17] and [18]; 3) fractional crystallization of mantle-derived mafic melts [19] and [20] and 4) Partial melting of an I-type granodioritic source [21]. The younger granitoids also attracted the interest of many authors because they are typically associated with anomalous concentrations of rare and some economically important elements such as Sn, W, Mo, U, Nb, Ta and Rb [10]. Uranium with an average concentration of 1.0 ppm in crust needs certain geologic environments to accumulate, however, its ore deposits occur in nearly every major rock type in the crust, and nearly all igneous, metamorphic and sedimentary processes are capable of its concentration or dispersion. As the solubility of monazite and xenotime remains very low regardless of a luminosity [22], phosphorus-rich peraluminous melts become saturated in monazite and xenotime at low REEs concentrations. The nature abundance and distribution of accessory minerals crystallizing from melt depend on four groups of parameters [22]: the trace element contents (a) chemical features (b) of the magma, (c) the degree of magma evolution, (d) and the physical chemical conditions of magma crystallization. This paper presents the results of detailed investigations involving geochemistry, mineralogy and spectrometric prospecting of granitoid rocks of the G. El Faliq area to identify the mode of occurrence of mineralization.

2. Geological Setting and Petrography

2. a. Field Observation

Gabal (G.) El-Faliq area is located between lat. 24° 35' and 24° 42' N and long. 34° 28' and 34° 35' E. The detailed field of the basement rocks (250 Km^2) is composed of ophiolitic mélange, gneisses, older and younger granitoids and post granitic dykes and veins (Fig.1).

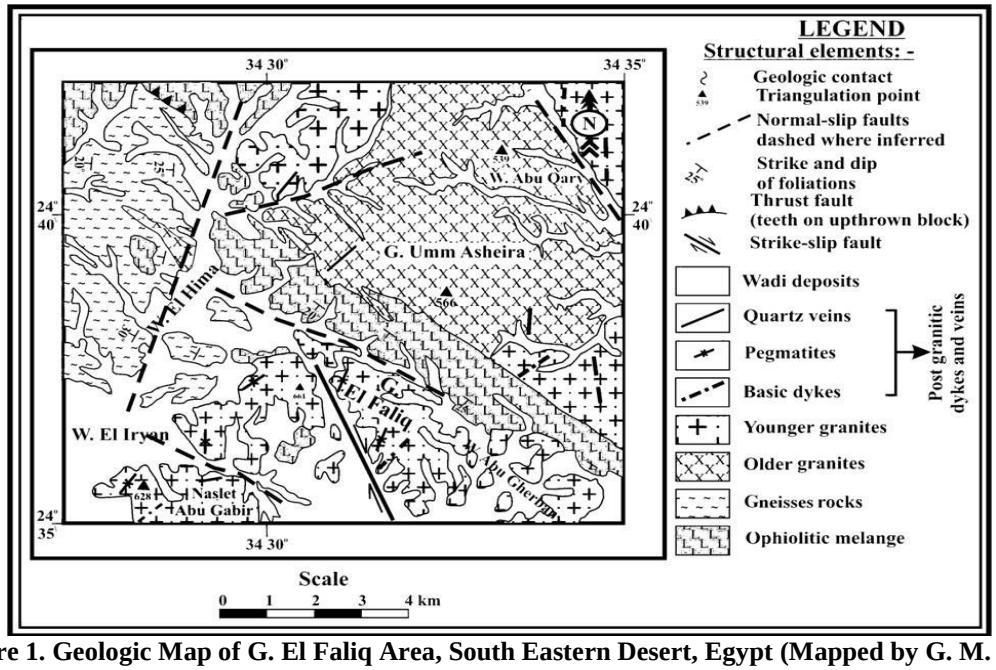

Figure 1. Geologic Map of G. El Faliq Area, South Eastern Desert, Egypt (Mapped by G. M. Saleh).

The older granitoids occur intruding along the contact between the ophiolitic mélange and the younger granitoids. They are characterized by relatively low to-medium topography (Fig.2a). They are cut and crossed by number of pegmatite and quartz veins as well as basic dykes, strike 125º with dip N 40º E/55º.

The younger granitoids in G. El Faliq area exposed in the east side of the G. El Faliq, Naslet Abu Gabir as well as northeast W. Abu Gherban (about 95 $km^{2)}$. They are characterized by low to moderate topography and form elongated mass in NW-SE direction. There are two varieties of younger granitoids in the study area. The first type is represented by monzogranites and alkali feldspar granites characterized by highly sheared and dissected by numerous faults (Fig. 2b). The second type is represented at the eastern and northeastern sides of the regional mapped area and emplaced along NW-SE trend, reached about 1.0-2.5 Km in length and 100- 350 m in width. Some basic dikes (NE-SW) cross-cut the alkali feldspar granites (Fig.2c). Some outer contacts of the younger granitoids are highly reddish colour due to the hematitization (Fig. 2d) or whitish due to kaolinization.

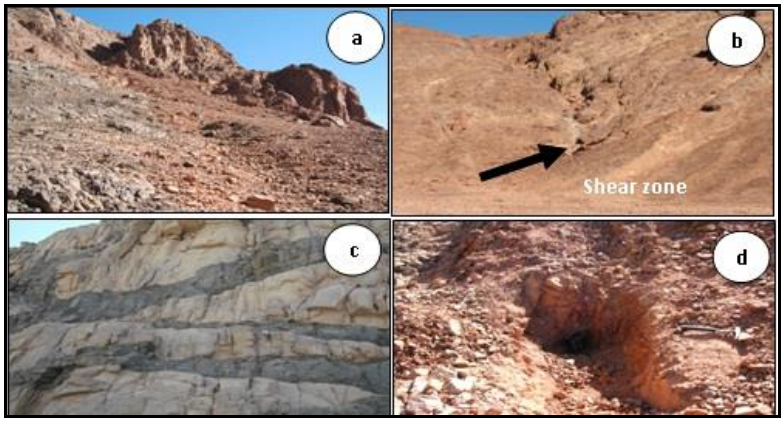

Figure 2. Photographs showing: (a) older granitoids characterized by relatively low to-medium topography, looking NE, (b) highly sheared granites and dissected by numerous faults, looking NE, (c) parallel basic dykes cross-cutting the younger granitoids, Looking NE and (d) hematitization along fractures in younger granitoids (trench No.1), looking NE, G. El Faliq area.

2. b. Modal Analyses and Nomenclature

The QAP modal analysis [23] shown in (Fig. 3) indicates that the older granitoids are either tonalites (4 samples) or/and granodiorites (2 samples) fields, whereas, the younger granitoids plotted in the monzogranite (3 samples) and alkali feldspar granite (9 samples) fields. All (18) samples contain two feldspars indicating crystallization under subsolvus condition (Tuttle and Bowen, 1958).

World Journal of Earth and Planetary Sciences
Vol. 1, No. 1, December 2014, pp. 1- 22
Available online at http://wjeps.com/

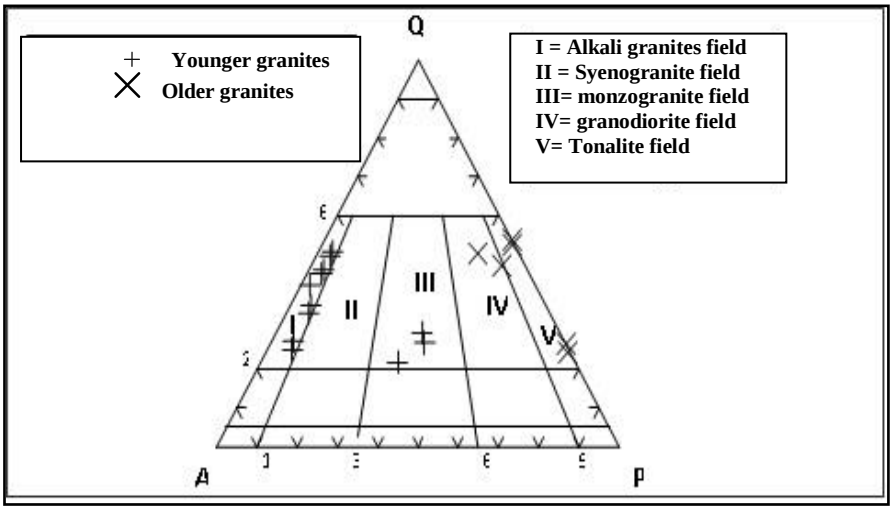

Figure 3. Modal quartz (Q) - alkali feldspar (A) - plagioclase (P) ternary diagram of the studied granitoid rocks of G. El Faliq area [23].

2. b.1.Older Granitoids

Tonalite is medium- to coarse-grained, light gray in colour, hard and massive. They are mainly composed of plagioclase (An_{33-36}), quartz, hornblende and biotite. Apatite, zircon, titanite and opaques occur in an order of decreasing abundance as accessories. Plagioclase occurs as euhedral to subhedral crystals of platy and blade-like forms. It exhibits albitic twining and zoning of normal type (Fig.4a). **Granodiorite** is medium- to coarse-grained, gray to pinkish gray colour, and exhibit hypidomorphic texture. They are mainly composed of plagioclase, quartz, orthoclase, microcline, biotite, hornblende and opaques. The accessory minerals are zircon and titanite. Plagioclase is the most dominant mineral and occurs as anhedral to subhedral prismatic crystals ranging in size from 5 x 2.6 mm to 1 x 0.2 mm. They are slightly altered, but the fresh crystals are oligoclase in composition (An_{20-26}) (Fig. 4b). Accessory minerals are mainly zircon that occurs as well-euhedral crystals associating or included in the main constituents (Fig.4c).

2. b. 2. Younger Granitoids

Monzogranite is massive, medium- to coarse-grained size, and buff to grayish buff in colour. They are mainly composed of potash feldspar, quartz, plagioclase (An_{13-20}) and biotite with subordinate amount of hornblende and muscovite. Zircon, garnet and opaques are accessory minerals. Microcline occurs as subhedral crystals showing its characteristic cross-hatched twining (Fig.5a). Orthoclase perthite is the dominant k-feldspar, occur as anhedral to subhedral crystals (6 X 3.5 to 3 X 1.5 mm size) exhibiting patchy perthite type. Biotite occurs as pleochroic flaky crystals, with X = yellowish brown and Y = Z = dark brown (Fig.5b).

Alkali feldspar granites are medium- to coarse-grained and ranging in colour from pinkish gray to dark pink. They are mainly composed of alkali feldspars, quartz, plagioclase, alkali amphiboles. Zircon, monazite and opaques are the accessory minerals. Potash feldspars are represented by string (Fig. 4d) and patchy type microcline perthite, as well as antiperthite of frequent K-feldspar exsolusion in albite crystals. Potash feldspars represent by microcline and predominantly orthoclase perthite (Fig.4e). Alkali amphiboles of riebeckite-arfvedsonite represent the main mafic minerals (Fig.4f) in the alkali feldspar granites.

Altered granites are massive and moderately to strongly altered exhibiting pinkish brown to brownish red colour. They are mainly composed of alkali feldspars and quartz with subordinate plagioclases, biotite and muscovite. Zircon, monazite and opaques occur as accessories. Secondary muscovite and kaolinite as well as secondary uranium minerals generally portray irregular shapes, and coated by iron opaques (Fig.4g). The altered granites of G. El Faliq area can be categorized according to its intense hematitization (Fig.4h) and/or kaolinitization processes into hematitized and/or kaolinitized granites.

3. Mineralogy

The heavy minerals have been investigated by using X-ray diffraction (XRD) techniques at the Nuclear Materials Authority of Egypt. X-ray diffraction technique was used to identify the unknown minerals using PHILIPS PW 3710/31 diffractometer with automatic sample changer PW 1775, (21 positions), scintillation counter, Cu-target tube and Ni filter at 40 kV and 30 mA. This instrument is connected to a computer system using X-40 diffraction program and ASTM cards for mineral identification. The samples were crushed and the size fraction of 0.063-0.5 mm was used. This size fraction was subjected to systematic mineral separation techniques using heavy liquids (Bromoform, 2.8 sp. gr.), magnetic fractionation using (Frantz Isodynamic Magnetic Separator) and microscopically handpicking mineral grains. The studied mineralization of G. El Faliq area can be classified into the following groups: 1) secondary uranium minerals, 2) niobium-tantalum minerals, 3) sulphide minerals and 4) accessory minerals.

1. Secondary Uranium Minerals

1. a. Uranophane [Ca $(UO_3)_2(SiO_2)_2(OH)_2$, $5H_2O$] is one of the secondary uranium minerals which are associated with hematite, zircon and columbite-tantalite minerals. An investigation of the uranophane grains under the binocular microscope showed that they are present as massive radiated and tufted aggregates as well as dense microcrystalline masses with different grades of canary to lemon- yellow colour, while it turns to the brownish yellow colour due to staining with hematite. It is identified by X-ray diffraction analyses (Fig. 5a).

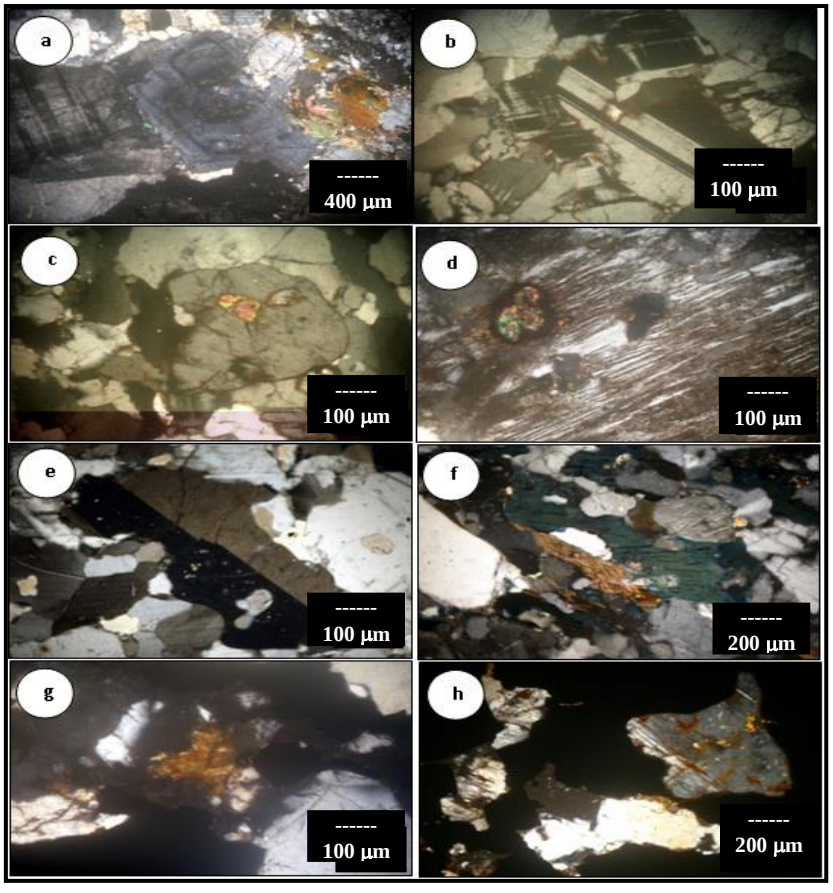

Figure 4. Thin section views in crossed Nichols showing mineral assemblages and textures in the G. El-Faliq granitoid rocks: (a) euhedral plagioclase crystals showing albitic twining and zonation in tonalite, (b) subhedral oligoclase crystals with broad lamellar twining associating microcline in granodiorite, (c) euhedral zircon crystal included in plagioclase in granodiorite, (d) anhedral crystal of string perthite stained by iron oxides and encloses zircon in alkali feldspar granite, (e) subhedral orthoclase crystal with Carlsbad twining associating quartz in alkali feldspar granite, (f) elongated crystals of riebeckite and arfvedsonite associating quartz and perthite in alkali-feldspar granite, (g) uranophane crystal associating quartz in altered granites and (h) plagioclase corroded by iron oxides due to hematitization in altered granites.

2. Niobium - Tantalum Minerals

2.a. Columbite [(Fe, Mn) (Nb, Ta) $_2$O6)] has been discovered in altered granitic rocks of G. El Faliq area. It occurs as black colored anhedral crystals with sub-metallic to resinous luster and dark red to black streak (Fig. 5b).

2. b. Euxenite [(Y. Ce, Ca, U, Th) (Nb, Ta, Ti) $_2$O $_4$] is a brownish black mineral with a metallic luster and reddish brown streak, its fracture is concoidal to sub-concoidal. X-ray diffraction pattern of euxenite mineral is shown in (Fig. 5c).

2.c. Fergusonite [(Y, Er) (Nb, Ta, Ti) O_4] is found in the altered granite as anhedral form with brown colour, its luster range from translucent in brown shades to glassy and the streak is grey to brown. Fergusonite mineral was observed in associated with zircon (Fig.5d).

3. Sulphide Minerals

3.a. Pyrite (FeS_2) occurs as isometric crystals that usually appear as cubes. Pyrite has pale-brassy to golden-yellow colour with metallic luster and black streak (Fig.6a).

3.b. Barite ($BaSO_4$) is colorless or milky white as well as greenish, reddish more yellow in colour on the periphery of the particles (Fig.6b).

4. Accessory Minerals

4. a. Allanite [(Ce, Ca, Y,) (Al, Fe)$_3$ (SiO_4)$_3$.OH is only recorded in the altered granites of G. El Faliq. It occurs as tabular, long prismatic crystals and has brown to black colour and pleochroic from pale brown to dark brown (Fig.7a).

4. b. Zircon ($ZrSiO_4$) is characterized by prismatic and bi-pyramidal crystals and has varying shades of honey colour due to the effect of radioactivity. Metamict zircon particles are also present, highly radioactive due to the presence of uranium and thorium (Fig. 7b).

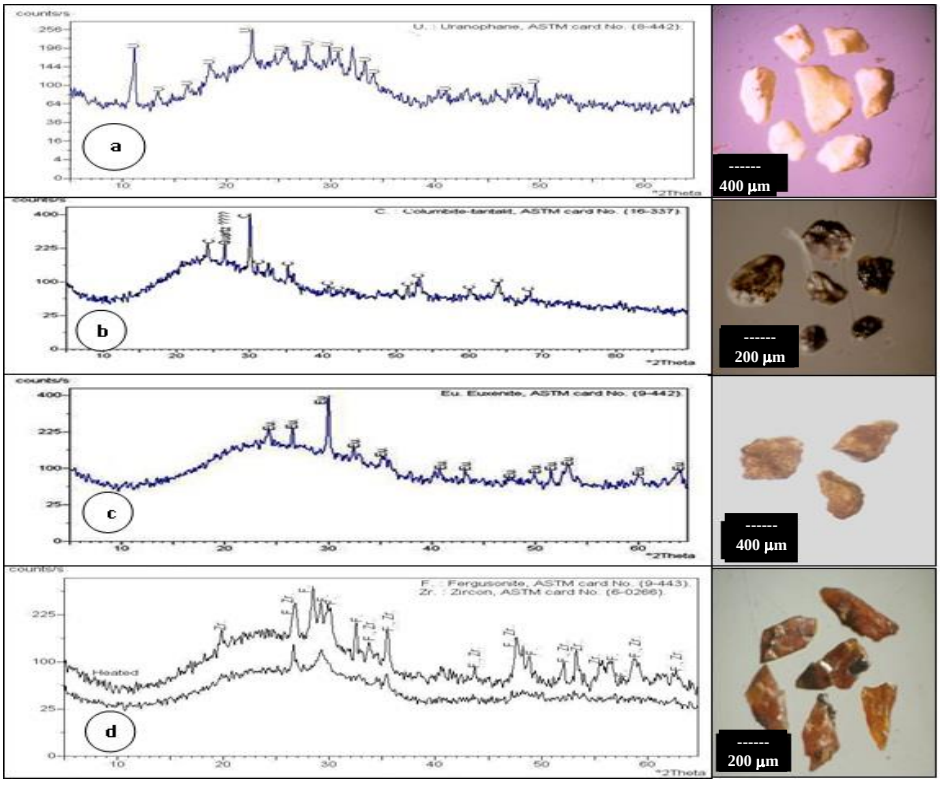

Figure 5. (a) X-ray diffractograms and photomicrographs of uranophane, (b) columbite, (c) euxenite and (d) fergusonite associated with zircon, G. El Faliq altered granites.

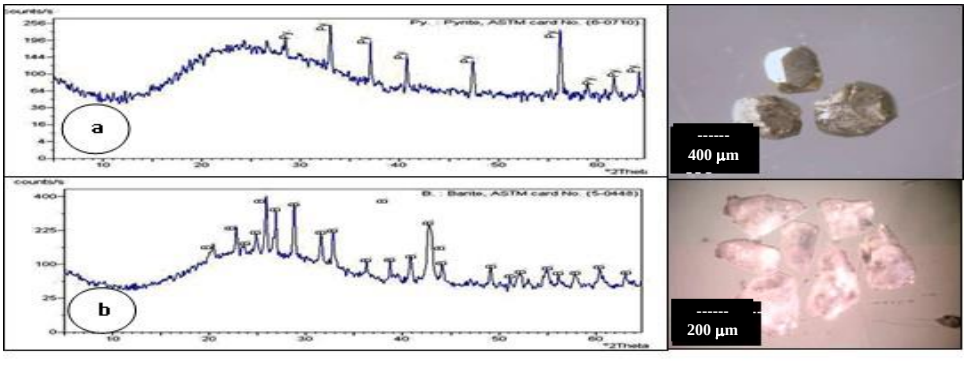

Figure 6. (a) X-ray diffractograms and photomicrographs of pyrite and (b) barite, G. El Faliq altered granites.

World Journal of Earth and Planetary Sciences
Vol. 1, No. 1, December 2014, pp. 1- 22
Available online at http://wjeps.com/

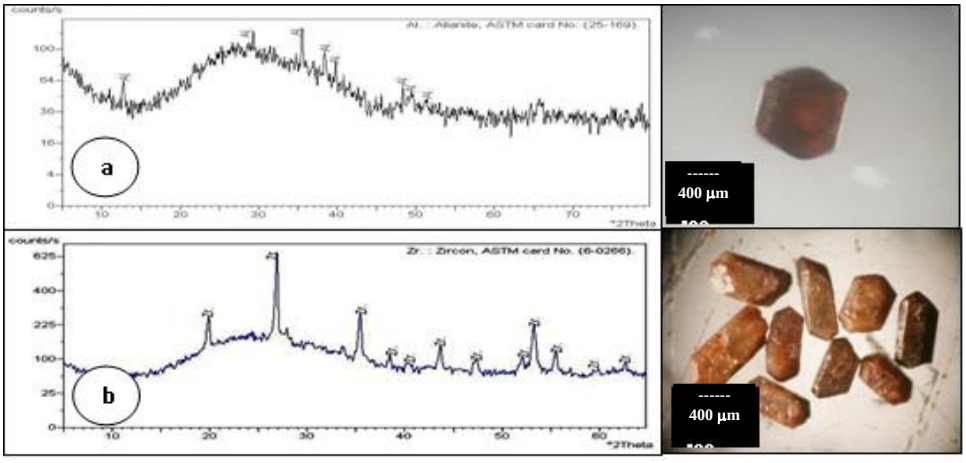

Figure 7. (a) X-ray diffractogram and photomicrograph of allanite and (b) zircon, G. El Faliq altered granites.

4. Whole Rock Geochemistry

4.1. Analytical Techniques

Twenty four (24) samples from the study area (8 alkali feldspar granites, 6 monzogranites, 5 granodiorites and 5 tonalites samples) were determined using conventional wet chemical technique [24] major oxides (in wt%), rare earth elements (REEs) (in ppm) and XRF technique for trace elements (in ppm). The REEs were analyzed using an ICP-AES spectrometer. Absolute accuracy has been assessed by comparison with international reference materials analyzed along with the samples and is generally better than 2% for major elements and 5% for trace elements. Loss on ignition (LOI) was calculated by heating about 3g of a rock powder in a porcelain crucible at about 1000˚c for 4 hours. Chemical data of the different rock types are given in Table (1).

4.2. Geochemical Classification

The studied older granitoids samples plot within the granodiorite and tonalite fields whereas younger granitoids samples plot in alkali feldspar granite and granite fields (Fig.8a). The normative composition Ab-Or-An on ternary diagram, shows where the analyzed older granitoid samples fall in granodiorite and tonalite fields respectively (Fig.8b). While the younger granitoid samples located in granite field close to Ab-Or side exhibiting their low An content with slight variation of Ab-Or ratio [25].

Table (1): Average of chemical composition of granitoid rocks of G. El-Faliq area, SED, Egypt.

Rock types	Older granitoids		Younger granitoids	
	Granodiorites	Tonalites	Alkali feldspar granites	Monzogranites
No.	(N =5)	(N =5)	(N =8)	(N = 6)
Average and range of major oxides (wt %)				
SiO_2	65.16 (64.12-66.23)	66.94 (65.31-69.42)	72.01 (70.56-73.40)	71.68 (70.70-72.70)
TiO_2	0.93 (0.70-1.43)	0.33 (0.002-0.50)	0.22 (0.03-0.30)	0.30 (0.20-0.44)

Al_2O_3	14.96 14.34-15.61	14.776 (13.49-16.40)	12.19 (11.83-12.60)	12.25 (11.13-13.98)
Fe_2O_3	2.094 (1.77-2.68)	1.878 (1.54-2.68)	1.65 (1.55-1.78)	1.67 (0.44-2.08)
FeO	2.83 (2.06-3.16)	2.038 (1.46-2.64)	1.59 (1.31-2.12)	2.50 (1.80-3.32)
MnO	0.07 (0.04-0.15)	0.25 (0.07-0.90)	0.13 (0.06-0.12)	0.07 (0.06-0.09)
CaO	3.89 (3.54-4.15)	3.96 (3.80-4.15)	1.25 (0.45-1.80)	1.37 (0.80-1.90)
MgO	2.76 (1.92-3.74)	2.46 (1.90-2.83)	0.59 (0.28-1.00)	0.90 (0.29-180)
Na_2O	3.45 (3.23-3.68)	3.43 (2.88-3.86)	4.42 (4.00-4.70)	3.67 (3.50-3.86
K_2O	2.72 (2.50-3.06)	1.25 (0.56-2.02)	4.96 (4.33-5.23)	4.20 (3.32-4.46)
P_2O_5	0.23 (0.01-0.55)	0.136 (0.01-0.63)	0.07 (0.01-0.12)	0.36667 (0.01-1.01)
L.O.I	0.92 (0.70-1.45)	0.794 (0.40-1.15)	0.41 (0.11-0.89)	0.67 (0.40-1.10)
Average and range of representative trace elements (ppm)				
Cr	55 (48-66)	45 (40-53)	56 (44-71)	38 (31-62)
Ni	6 (4-6)	6 (5-6)	7 (4-10)	18 (7-31)
Cu	41 (31-64)	50.6 (46-66)	31.25 (25-39)	14 (10-29)
Zn	168.2 (138-193)	56 (44-63)	52.63 (27-148)	127 (27-205)
Zr	1241.2 (1011-1663)	82.2 (65-98)	273 (121-831)	1791 (1132-2792)
Rb	79.8 (76-87)	15 (14-17)	98.38 (58-125)	85 (42-141)
Y	56.2 (44-54)	5.6 (5-7)	87.25 (39-254)	164.17 (59-342)
Ba	701 (670-763)	699.6 (560-851)	186.63 (71-550)	374 (320-591)
Pb	50.2 (44-54)	41.4 (17-76)	14.38 (6-31)	13.83 (2-42)
Sr	1558.4 (1164-1884)	144 (122-174)	361.13 (17-1437)	667.17 (180-1956)
Ga	53.8 (39-76)	20 (6-32)	20.75 (2-70)	24.33 (12-28)
V	9.8 (5-12)	26 (24-30)	4.5 (2-12)	6.33 (6-7)
Nb	57 (48-70)	4.6 (4-6)	35.38 (3-111)	41 (8-151)

4.3. Magma Type

Alumina saturation diagram (Figs. 9a and b) show that the data points of the granodiorites are of metaluminous character, while tonalites fall between peraluminous and metaluminous fields. The alkali feldspar granites fall mainly in peralkaline character except one sample has peraluminous character. On the other hand, monzogranite samples fall in metaluminous field except two samples lies between peraluminous and metaluminous fields.

AFM diagram (Fig.9c) shows that older and younger granitoid samples plot in the calc-alkaline trend. It can be noticed that the younger granitoid is closed to the alkali apex. This indicates that the studied granitoid rocks of G. El Faliq area originate from calc-alkaline magmas characteristic of orogenic belts [26].

The K_2O-Na_2O-CaO diagram (Fig.9d) is drawn to distinguish the calc-alkaline character of rocks [27] and [28]. The examined older granitoid samples plot near the CaO-Na_2O side, whereas the samples of younger granitoids plot near the K_2O-Na_2O side. Generally all samples of the older and younger granitoids lie in clac-alkaline field [28].

The studied granitoid rocks fall in the I-type granite field (Figs.9e and f) except one sample of tonalite plot in S-type field according to [29]. The occurrence of magnetite and metaluminous to mildly peraluminous characters of the studied granitoids are consistent with their designation as I-type granitoids.

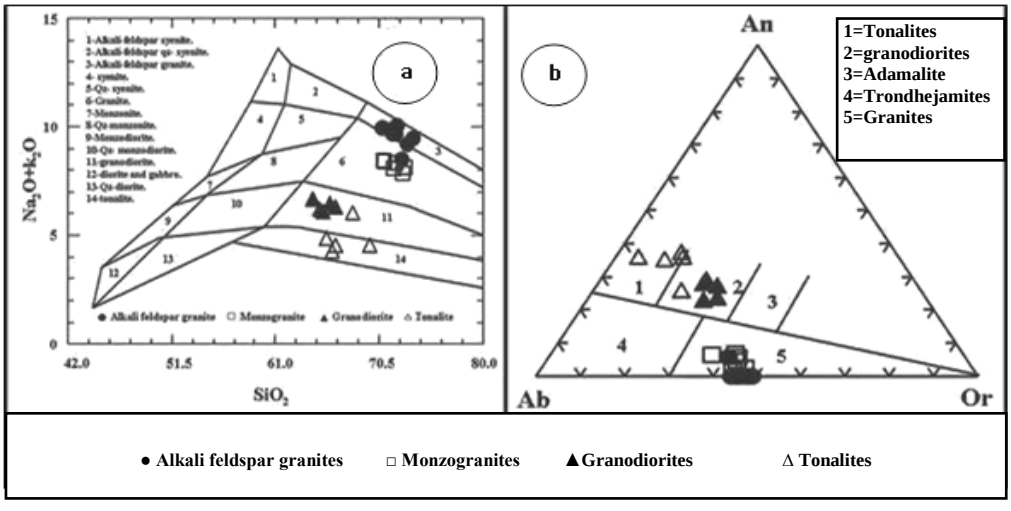

Figure 8. (a) Chemical classification of granitoid rocks using diagram [30] and (b) Nomenclature of granitoid rocks[25].

Plotting normative Qz-Ab-Or values on the ternary diagrams (Figs.9g and h) show the water-vapor pressures up to 3K-bar [31] and 5 to 10 K-bars [32], whereas the diagram (Fig.9h) shows the temperature isotherms for crystallization rocks. The granitoid rocks especially the granodiorite and monzogranite fall in a relatively 2-3 K-bar and temperature ranging about 760-800^{o}C, while tonalite fall in low water-vapor pressure ranging from 1-2 K-bar and temperature ranging about 760-840 ^{o}C indicating that, they were possibly formed at low levels in the crust. The alkali feldspar granite fall in high water-vapor pressure, varying between 3-10 K-bar and high temperature ranging about 800 ^{o}C indicating that, they were possibly formed at deep levels in the crust.

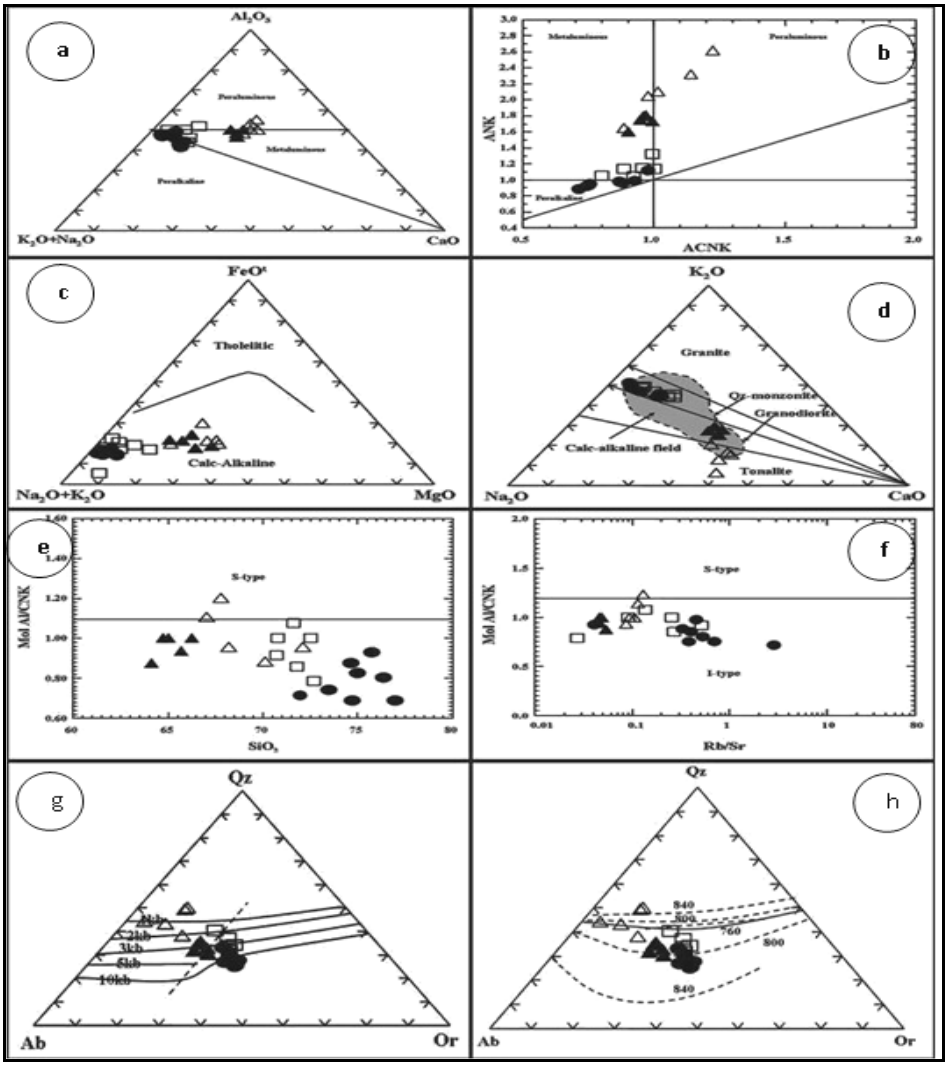

Figure 9. (a) molecular proportions of Al_2O_3-Na_2O-K_2O [33], (b) $Al_2O_3/(Na_2O+K_2O)$ versus $Al_2O_3/(CaO+Na_2O+K_2O)$ diagram [34], (c) AFM diagram after [26], (f) K_2O-Na_2O-CaO diagram of [27] and [28], (d) $Al_2O_3/(Na_2O + K_2O + CaO)$ ratio against SiO_2% [29], (e) $Al_2O_3/(Na_2O + K_2O + CaO)$ ratio against Rb/Sr ratio [29], (f) Normative Qz-Ab-Or ternary diagram. The dashed line represents the variation in position of the minimum melting points in the granite system at different water vapor pressures and (g and h) Normative composition Qz-Ab-Or isobaric equilibrium ternary diagram [31] (Symbols as in Fig. 8).

4.4. Tectonic Setting

Nb versus Y variation diagram with fields [35] is shown in (Fig.10a). Most samples of alkali feldspar granite, monzogranite and granodiorite fall in the field of within plate granites except some samples of monzogranite which fall in ocean ridge granites and tonalite samples in volcanic arc granite. Rb versus (Nb+Y) [35] variation digram. In the (Fig.10b) it can be noticed that, most samples of alkali feldspar granite, monzogranite and granodiorite fall in the field of within plate granites and tonalite samples in volcanic arc granites.

4.5. Petrogenesis

The older granitoid rocks (granodiorite and tonalite) and younger granitoids (alkali feldspar granite and monzogranite) samples located between mantle line (K/Rb=1000) and core line (K/Rb=100) K/Rb diagram

(Fig.10c). These indicate that the granitoid rocks of G. El Faliq area were generated from source regions depleted in Rb or were generated by partial melting in the lower or upper mantle [36] and [37].

[38] reported that the average ratio K/Ba ratio for the crust is 65. The studied older granitoid rocks plot below average crustal ratio, exhibiting lower K_2O content and they have (K/Ba >65). The younger granitoid rocks located above average crustal ratio and they have (K/Ba <65), they display Ba depletion with K_2O enrichment which indicates the involvement of a second process coupled with the crystal fractionation and leading to depletion of Ba with differentiation (Fig.10d).

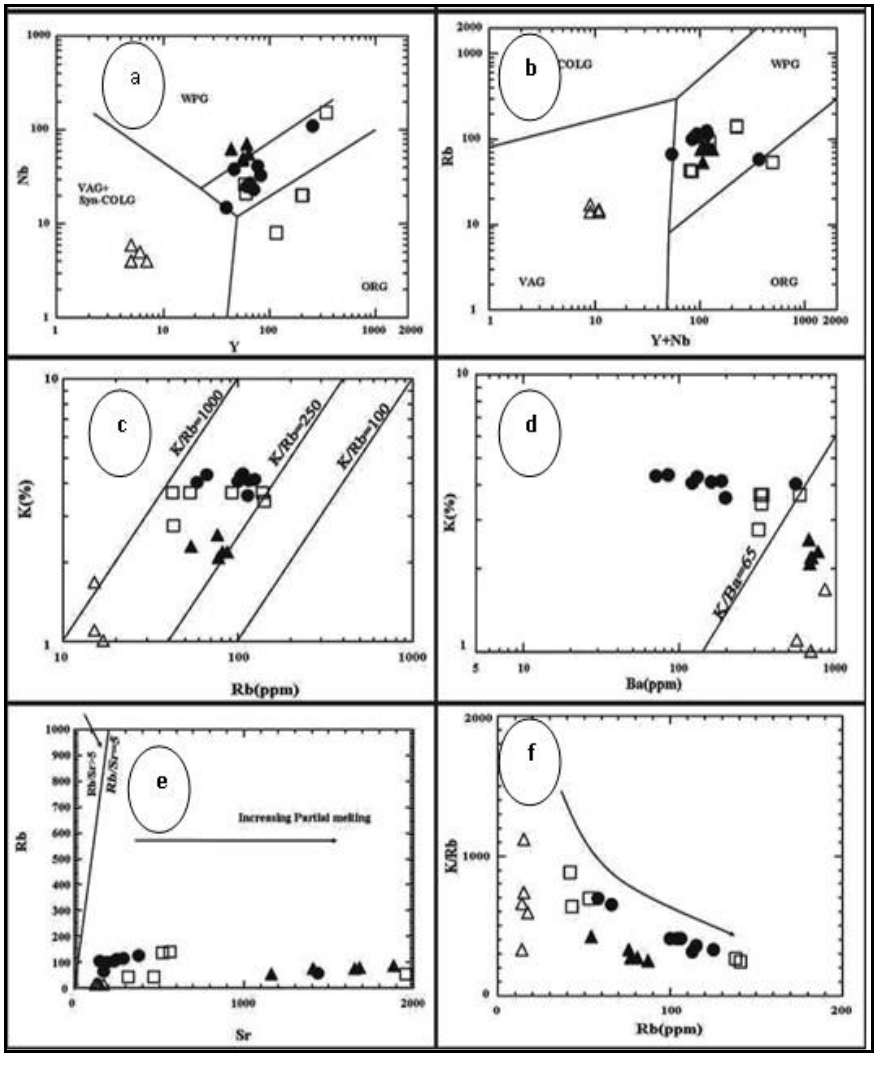

Figure 10. (a) Y versus Nb discrimination diagram [35], (b) Rb versus (Y+Nb) discrimination diagram [35], (c) K-Rb diagram, after [39], crustal K/Rb ratios after [40], (d) Ba-K variation diagram [38], (e) Sr versus Rb diagram for granitoid rocks and (f) K/Rb versus Rb diagram for granitoid rocks, (Symbols as in Fig. 8).

Depletion of Sr with differentiation from the studied older granitoids toward the younger granitoid samples is shown on the Sr-Rb diagram (Fig.10e). The K/Rb ratio against Rb (Fig.10f) is useful parameters for comparing of different sources. This plot shows the same trend for all members of petrogenetic sequences of studied granitoid rocks. The curved relationships on the diagrams could suggest that crystal fractionation was the dominating process during magmatic differentiation.

4.6. Geochemistry of Altered Granites

The complete chemical analyses of the altered granitic rocks (6 samples) are given in Table.2. A comparison between the average of the major oxides of the fresh samples of younger granitoids shows that, the younger granitoids are enriched in SiO_2, Na_2O and K_2O but depleted in TiO_2, Al_2O_3, Fe_2O_3, FeO, MnO, CaO, MgO and P_2O_5 relative to the altered granites. Also, with regards to trace elements they are enrich in Sr and depleted in Ni, Zn, Zr, Y, Ba, Nb, U and Th (Figs.11a and b). According to [41] the samples of altered granites are located in argillation field (Fig.11c) toward the K-metasomatism and this is consistent with the formation of kaolinite minerals as the product of alteration. This argillation represents the main alteration process that affected the studied granitic samples. Altered granite samples are plotted on AKF ternary diagram (Fig.11d) after [42]. It shows that all samples are argillic in nature.

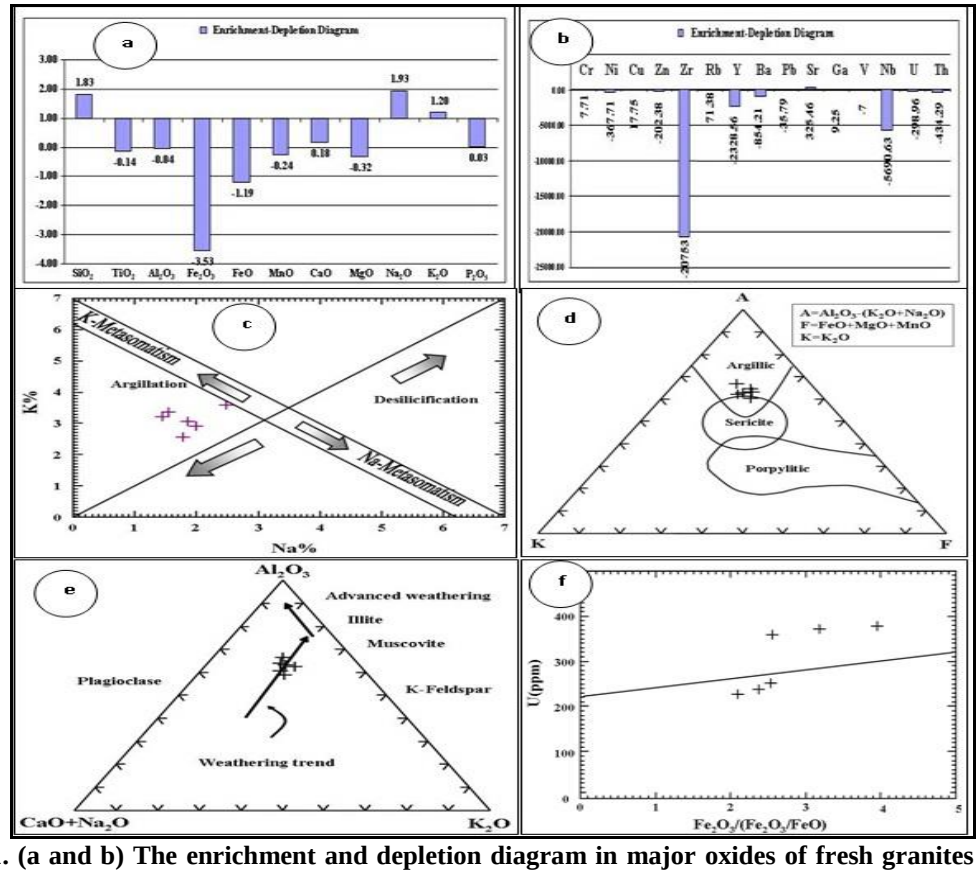

Figure 11. (a and b) The enrichment and depletion diagram in major oxides of fresh granites related to altered granites, (c) K-Na variation diagram, showing the alteration type [41], (d) AKF ternary diagram [42], (e) Al_2O_3-($CaO+Na_2O$)-K_2O ternary diagram, showing the weathering trend [43] and [44] and (f) U versus Fe_2O_3/ (Fe_2O_3/FeO) variation diagram of the altered granites.

The weathering trends of the granitic rocks displayed on (Na_2O + CaO)-Al_2O_3-K_2O triangular diagram Fig.(11e), [43] and [44]. The initial stages of weathering form a trend parallel to the (Na_2O + CaO)-Al_2O_3 side of the diagram, whereas advance weathering shows a marked loss in K_2O compositions and more towards the Al_2O_3 apex. The Figure shows that all samples plot toward Al_2O_3 apex and the altered granite samples are more depleted in K_2O and Na_2O + CaO content. The abundant hematite crystallization in the altered granites, which is reflected in the obvious increase of Fe_2O_3, also reflect the oxidation state. The relationship of U (ppm) and the oxidation state is manifested by the ratio Fe_2O_3/ (Fe_2O_3/FeO) portrayed on (Fig. 11f).

Table (2): Chemical analyses of major oxides (wt. %) and trace elements (ppm) for altered granitic rocks, G. El-Faliq area, SED, Egypt.

Altered granites N = 6							Average		
Major Oxides	1	2	3	4	5	6	A	B	C
SiO_2	70.84	69.5	71.5	68.7	71.02	69.15	66.05	71.87	70.12
TiO_2	0.34	0.3	0.4	0.25	0.31	0.54	0.63	0.25	0.36
Al_2O_3	13.23	12.85	10.3	12.08	11.12	13.83	14.87	12.22	12.24
Fe_2O_3	4.31	5.2	4.9	6.33	6.64	3.71	1.99	1.66	5.18
FeO	2.5	2.55	2.1	3.18	3.96	2.37	2.43	1.98	2.78
MnO	0.35	0.72	0.17	0.04	0.48	0.43	0.16	0.11	0.37
CaO	1.62	1.04	1.03	0.63	0.87	1.23	2.61	0.72	1.07
MgO	0.59	1.2	1	0.7	0.28	1.64	3.93	1.30	0.90
Na_2O	2.09	2.7	2.5	2.4	1.94	3.35	3.44	4.10	2.50
K_2O	4.05	3.5	3.7	3.1	3.87	4.33	1.99	4.63	3.76
P_2O_5	0.05	0.06	0.03	0.02	0.08	0.02	0.18	0.20	0.04
L.O.I	1.15	1.1	1.25	1.9	1.18	0.77	0.86	0.52	1.23
Total	101.12	100.72	98.88	99.33	101.75	101.37	99.14	99.56	100.53
Trace elements (ppm)									
Cr	50	53	47	47	47	45	50	48	48
Ni	223	228	140	518	588	549	6	11	374
Cu	10	10	10	16	17	18	46	24	14
Zn	157	156	121	361	367	368	112	85	255
Zr	2902	2782	1775	>10000	40058	>10000	662	923	21026
Rb	39	41	28	17	18	19	47	93	27
Y	1776	1762	1069	462	4744	4670	31	120	2414
Ba	685	699	646	1317	1367	1351	700	267	1011
Pb	24	22	4	86	79	86	46	14	50
Sr	57	55	34	23	22	23	851	492	36
Ga	21	22	17	3	2	4	37	22	12
V	9	9	8	14	15	14	18	5	12
Nb	3246	3341	1858	8611	8611	8789	31	38	5743
U	251	360	230	373	384	240	n. d	7	306
Th	252	548	414	571	439	432	n. d	8	443

A = Average of older granitoids. B = Average of younger granitoids. C = Average of altered granites. n. d. = not detected.

4.6.1. Rare earth elements (REEs)

The average normalized REEs patterns of G. El Faliq altered granites display low to moderate fractionated REEs pattern (Fig.12) relative to chondritic values from [45], where the averages $(La/Yb)_n$ = 2.14 have slight enrichment in the LREEs (1759.30), where the averages $(La/Sm)_n$= 4.28 and the average of $(Eu/Sm)_n$ is 0.38 respectively (Table.3). It is concluded that G. El Faliq altered granites have moderate negative Eu anomaly (Eu/Eu^*= 0.60), this may reflects the slight difference in their origin [46]. This difference can be interpreted as due to the greater effect and higher oxygen activity of the melt, which is related to volatile saturation (higher oxidation state) in case of the melt that formed the granitic melt. The oxygen activity of the melt would be sufficiently high to keep Eu at the trivalent state and thus keep its incorporation into accumulating plagioclase [47]. The marked enrichment of the average of ∑HREEs (2060.91) relative to the

average of ∑LREEs (1774.66) where the averages of $(Tb/Yb)_n$ recorded as 0.81 is most likely to indicate the retention of both hornblende and zircon in the source rocks relative to the melts that formed these rocks. Generally, it can be suggested that G. El Faliq altered granites originated from different sources.

Table (3): The REEs contents of the altered granitic rocks, G. El Faliq area,SED, Egypt.

Altered granites							
Samples	**1**	**2**	**3**	**4**	**5**	**6**	**Average**
La	**32.75**	**796**	**285.15**	**15.42**	**158.95**	**405.71**	**282.33**
Ce	**110.3**	**1765.95**	**646.5**	**45.44**	**378.4**	**905.70**	**642.05**
Pr	**19.35**	**209**	**74.8**	**4.2**	**47.08**	**106.6**	**76.84**
Nd	**93.72**	**2029**	**510.35**	**13.5**	**302.04**	**1021.25**	**661.64**
Sm	**34.2**	**259.18**	**90.85**	**1.55**	**62.53**	**130.37**	**96.45**
Eu	**4.5**	**42.8**	**13.9**	**0.2**	**9.2**	**21.5**	**15.35**
Gd	**141.65**	**523.5**	**141.05**	**3.2**	**141.35**	**263.35**	**202.35**
Tb	**42.01**	**187.68**	**38.32**	**0.56**	**40.17**	**94.12**	**67.14**
Dy	**238.65**	**1571.1**	**303.65**	**4.47**	**271.15**	**787.79**	**529.47**
Ho	**56.3**	**446.61**	**95.95**	**1.1**	**76.13**	**223.86**	**149.99**
Er	**157.1**	**1219.54**	**188.88**	**3.45**	**172.99**	**611.50**	**392.24**
Tm	**21.95**	**141.72**	**28.4**	**0.42**	**25.18**	**71.07**	**48.12**
Yb	**128.6**	**1177.5**	**150.3**	**2.7**	**139.45**	**590.1**	**364.78**
Lu	**15.5**	**1197.7**	**13.65**	**0.41**	**14.58**	**599.06**	**306.82**
∑ REEs	**1097.6**	**11569.3**	**2584.8**	**100.6**	**1841.17**	**5834.95**	**3838.06**
∑LREEs	**294.82**	**5101.93**	**1621.55**	**80.31**	**958.2**	**2591.13**	**1774.66**
∑HREEs	**801.76**	**6465.35**	**960.2**	**16.31**	**880.98**	**3240.83**	**2060.91**
LREEs/HREEs	**0.36**	**0.78**	**1.67**	**4.91**	**1.015**	**2.85**	**1.93**
$(La/Yb)_n$	**0.25**	**0.68**	**1.9**	**5.71**	**1.08**	**3.20**	**2.14**
$(La/Sm)_n$	**0.96**	**3.07**	**3.14**	**9.95**	**2.05**	**6.51**	**4.28**
$(Gd/Lu)_n$	**9.14**	**0.44**	**10.33**	**7.8**	**9.74**	**4.12**	**6.93**
$(Gd/Yb)_n$	**1.1**	**0.44**	**0.94**	**1.19**	**1.02**	**0.82**	**0.92**
$(Tb/Yb)_n$	**0.15**	**0.72**	**1.16**	**0.94**	**1.31**	**0.72**	**0.81**
$(Eu/Sm)_n$	**0.35**	**0.44**	**0.40**	**0.34**	**0.39**	**0.34**	**0.38**
$(Eu)_n$	**77.59**	**737.93**	**239.66**	**3.4**	**158.62**	**370.69**	**264.64**
Eu*	**392.52**	**317.83**	**638.4**	**157.75**	**530.2**	**1044.97**	**514.61**
Eu/ Eu*	**0.20**	**2.32**	**0.38**	**0.02**	**0.30**	**0.35**	**0.60**

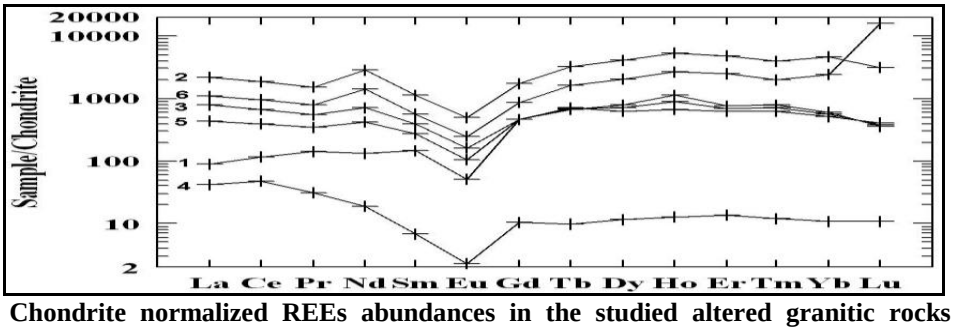

Figure 12. Chondrite normalized REEs abundances in the studied altered granitic rocks using the normalizing values of [45].

5. Spectrometric Prospecting

In situ γ-ray spectrometry measurements have been carried out using a UG-512 spectrometer with a 3 x 3 sodium iodide (Thalium) [NaI(TI)] crystal detector. Before the field measurements the spectrometer was calibrated on concrete pads containing known concentrations of K, U and Th. This calibration provide for correction of the measured K, eU and eTh. The term "equivalent" or its abbreviation "e" is used to indicate that

equilibrium is assumed between the radioactive daughter isotope monitored by the spectrometer, and its relevant p arent isotope. γ-rays emitted by ^{214}Bi at 1.76 MeV were measured for ^{238}U and gamma rays emitted by ^{208}TI at 2.41 MeV were measured for ^{232}Th.Within the detector, an internal ^{137}Cs source which allows the spectrometer to automatically maintain system stability is measured over a large body of water.

5. a. Distribution of Radio-elements in Granitoid Rocks.

The relationship between the eU , eTh contents, eU/ eTh and eU - (eTh/3.5) among the younger granitoids indicate slightly positive correlation while the variation between the eU/eTh ratios and eTh contents (Fig.13) shows negative linear correlation suggesting an enrichment of uranium relative to thorium where uranium had been added to these younger granitoids. Whereas, the relationship between eU with eTh , the eU with eU/eTh contents and eU- (eTh/3.5) among the altered granites (shear zone I and shear zone II) reflect a direct relation (Figs.14 and 15), the relation between eTh and eU/eTh and the eU with K% shows random and negative linear distribution, that means the eU/eTh ratio tends to increase with uranium mobilization and post magmatic redistribution in anomalies shear zones I and II of G. El Faliq, uranium had been added to these granites and this could be a favorable economic criterion to zone/categorize with the G. El Faliq area [48].

5. b. Equilibrium State of Radioactive Anomalies

The D-factor (U/eU) is equal to the ratio of the chemically determined uranium/radiometrically measured uranium [49]. If this factor is approximately unity, it indicates addition or removal of uranium respectively [50]. From the D-factor of the G. El Faliq samples of the altered granites presented in Table (4) and (Fig. 16), it is clear that chemical uranium is less than the radiometric uranium in all of the samples, which reflects disequilibrium due to the removal of uranium.

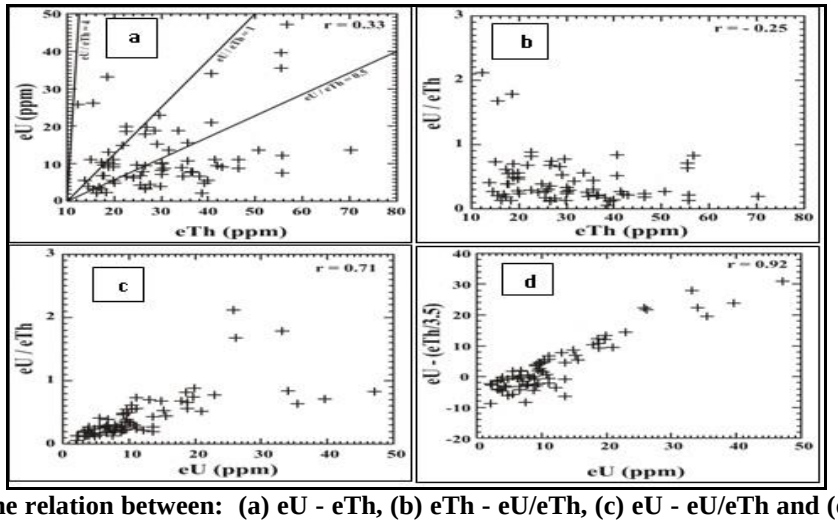

Figure 13. The relation between: (a) eU - eTh, (b) eTh - eU/eTh, (c) eU - eU/eTh and (d) eU- (eTh/3.5) of younger granitoidS, G. El Faliq , SED, Egypt.

World Journal of Earth and Planetary Sciences
Vol. 1, No. 1, December 2014, pp. 1- 22
Available online at http://wjeps.com/

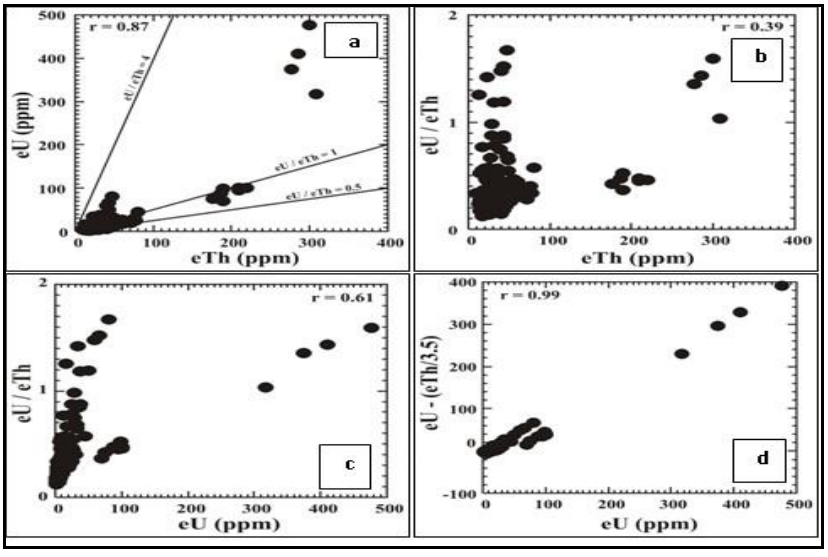

Figure 14. The relation between (a) eU - eTh, (b) eTh - eU/eTh, (c) eU - eU/eTh and (d) eU- (eTh/3.5) of altered granites (Shear zone I), G. El Faliq area, SED, Egypt.

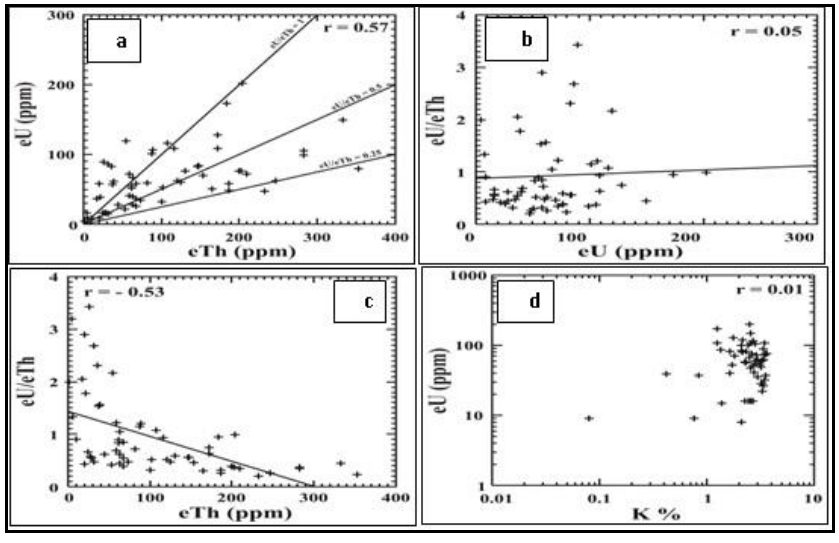

Figure 15. The relation between (a) eU - eTh, (b) eU - eU/eTh, (c) eTh - eU/eTh and (d) K-eU of altered granites (Shear zone II), G. El Faliq area.

Table (4): Results of U-spectrometric (eU) and U- chemical analyses of G. El Faliq altered granites, SED, Egypt.

Sample No	eU (ppm)	U (ppm)	U/eU	Sample No	eU (ppm)	U (ppm)	U/eU
1	510	251	0.49	11	345	225	0.65
2	590	360	0.61	12	330	220	0.67
3	350	230	0.66	13	240	147	0.61
4	650	373	0.57	14	280	142	0.51
5	390	384	0.98	15	390	235	0.60
6	380	240	0.63	16	470	220	0.47
7	270	150	0.56	17	485	233	0.48
8	295	210	0.71	18	520	264	0.51
9	265	149	0.56	19	610	311	0.51
10	300	227	0.76	20	550	242	0.44

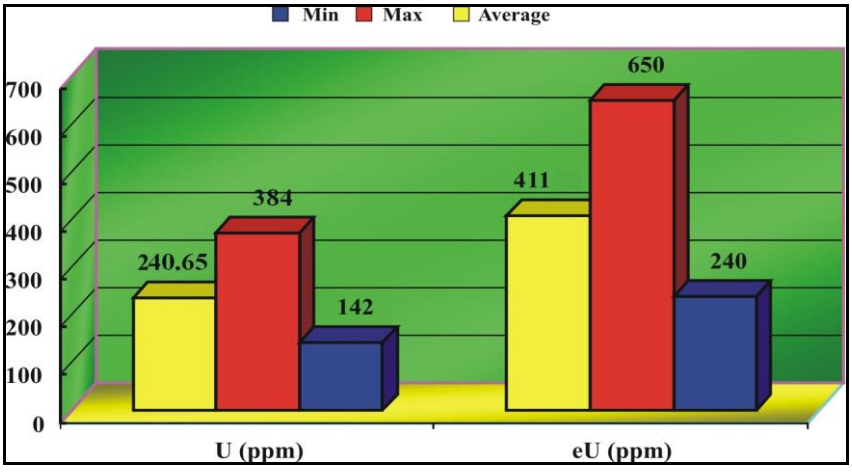

Figure 16. Bar diagram showing the comparison between average of U-chemistry (ppm) and U-radiometry (ppm) G. El Faliq altered granites.

Conclusions

1. The G. El-Faliq area is composed of ophiolitic mélange, gneisses, older and younger granitoids and post granitic dykes and veins. The younger granitoids are exposed in the east side of the G. El Faliq area especially in Naslet Abu Gabir and northeast W. Abu Gherban. Petrographically, they are mainly composed of potash feldspar, quartz, plagioclase, biotite and hornblende. Accessory minerals are represented by zircon, garnet and opaques. Altered granites are characterized by intense hematitization and kaolinitization. Microscopically, they are mainly composed of alkali feldspars and quartz with subordinate plagioclases, biotite and muscovite. Zircon and opaques in addition to monazite occur as accessories.

2. Geochemically, the older granitoids are peraluminous to metaluminous granites, while the younger granitoids are calc-alkaline and metaluminous to peralkaline granites. The altered granites show argilic facies with a relative depletion in K_2O and Na_2O + CaO.The average normalized REEs patterns of the altered granites display low to moderate fractionated REEs pattern relative to chondritic values from Hasken *et al.*, (1968). Generally, it can be suggested that G. El Faliq altered granites originated from different sources.

3. The mineralization of G. El Faliq can be classified on the basis of mode of occurrence and lithological associations into: a) secondary uranium minerals (uranophane), b) niobium-tantalum minerals (columbite, euxenite and fergusonite), c) sulphide minerals (pyrite and barite) and d) accessory minerals (allanite and zircon) as confirmed by XRD analysis.

4. The radiometric investigation suggests that the studied granitoid are uraniferous granites, which could be considered as favorable environments for uranium deposition containing high eU and eTh. The origin of secondary uranium mineralization is mainly related to alteration of primary minerals by the action of oxidizing fluids, mobilization of uranium and then redeposition in other forms. Redistribution by circulating meteoric waters might have taken place.

Acknowledgments

The authors wish to thank the Prof. Dr. M. E. Ibrahim, Head of the Research Sector, Nuclear Materials Authority, Egypt and Dr. Magda A. Khalaf for interest as well as for help during field work and for guidance during the progress of the manuscript.

References

[1] Kröner A (1984). Late Precambrian plate tectonics and orogeny: a need to redfine the term Pan-African. In (Klerkx, J. and Michot, J. eds.) Geologie Africane. African Geology: 23-28.

[2] El Ramly MF, Akaad MK (1960). The basement complex in the Central Eastern Desert of Egypt between latitudes 24° 30 and 25° 4^N Geol. Surv. Egypt, paper No. 8: 35p.

[3] El Sokkary AA, El Shatoury HM, Sayyah TA, Attawiya MY, Assaf HS (1976). Contribution to the geochemistry of some granitic rocks from Egypt. Erde. 35: 335-343.

[4] Akaad MK, Noweir AM (1980). Geology and lithostratigraphy of the Arabian Desert orogenic belt of Egypt between lat. 25 35 and 26 30 N. Inst. Applied Geol., King Abdul Aziz Univ., Jeddah 3(4): 127-135.

[5] El Gaby S, Habib MS (1982). Geology of the area SW of Port Safaga, with especial emphasis on the granitic rocks, Eastern Desert, Egypt. Ann. Geol. Surv. Egypt. 12: 47 - 71.

[6] Hussein AA, Ali MM, El Ramly MF (1982). A proposed new classification of the granites of Egypt; Jour. Volcan. Geoth. Res.;Vol. 14: 187-198.

[7] El Gaby S (1975). Petrochemistry and geochemistry of some granite from Egypt. Neues Jahrbuchfur Mineral., 124: 147 - 189.

[8] Ragab AI, Meneisy MY, Diab MM (1989). Petrology and petrogensis of the older and younger granitoids of Wadi Bezah area, Central Eastern Desert, Egypt. Jour. Afr. Earth. Sci., V. 9, No. 2: 303-315.

[9] Hassan MA, Hashad AH (1990). Precambrian of Egypt. In: Said R. (ed): The Geology of Egypt. Balkema, Rotterdam: 201-245.

[10] Noweir AM, Sewifi BM, Abu El Ela AM (1990). Geology, petrography, geochemistry and petrogenesis of the Egyptian younger granites. Qatar Univ. Sci. Bull, 10: 363-393.

[11] Abdel Rahman AM, Martin, RF (1990). The Mount Gharib A-type granite, Nubian Shield: petrogenesis and role of metasomatism at the source. Contrib. Miner. and Petro.;Vol. 104: 173-183.

[12] Saleh GM (2001). Evolution of Pan-African A- and I-type granites from south eastern Desert, Egypt: Inferences from geology, geochemistry and mineralization; International Geology Review; Vol. 43: 548-564.

[13] Abdel Rahman AM, Martin RF (1987). Late-Pan African magmatism and crustal development in northeastern Egypt. Geol. Jour.,Vol. 22:281-301.

[14] Funes H, El Sayed MM, Khalil SO, Hassanen MA (1996). Pan-African magmatism in the Wadi El Imra district, Central Eastern Desert, Egypt: geochemistry and tectonic environment; Jour. Gol. Soc. Lond.;Vol. 153: 605-818.

[15] Ibrahim ME, Saleh GM, Abd El Naby HH (2001). Uranium mineralization in the two mica granite of Gabal Ribdab area, South Eastern Desert, Egypt. Applied Radiation and Isotopes;Vol. 55: 861-872.

[16] Abd El Naby HH , Saleh GM (2003). Radioelement distributions in the Proterozoic granites and associated pegmatites of Gabal El Fereyid area, Southeastern Desert, Egypt. Applied Radiation and Isotopes.Vol. 59: 289-299.

[17] El Gaby S, List FK, Tehrani R (1988). Geology, evolution and metallogenesis of the Pan-African Belt in Egypt. In (S.El Gaby, S.&R.D.Greiling, R.D., eds). The Pan-African Belt of the North East Africa and Adjacent Areas. Vieweg Verlag, Wiesbaden: 17- 68.

[18] El Gaby S, List FK, Tehrani R (1990). The basement complex of the Eastern Desert and Sinai". In (Said, R. ed.) The Geology of Egypt. Balkama-Rotterdam Brookfield: 175-184.

[19] Stern RJ, Gottfried DY (1986). Petrogenesis of late Precambrian (575-600 Ma) bimodal suite in north-east Africa; Contrib. Miner. and Petr.; Vol. 92: 492-501.

[20] Dawood YH, Saleh GM, Abd El Naby HH (2005). Effects of hydrothermal alteration on Geochemical characteristics of the El Sukkari granite,central Eastern Desert, Egypt. International Geology Review; Vol. 47: 1316-1329.

[21] El Sayed MM (1998). Tectonic setting and petrogenesis of the Kadabora pluton: A late Proterozic anorogenic A-type Younger Granitoids; Chem. Erde;Vol. 58: 38-63.

[22] Pagel M., (1981). The mineralogy and geochemistry of uranium, thorium, and rare-earth elements in two radioactive granites of the Vosges, France. Mineral. Mag., 46: 149-161.

[23] Streckeisen A (1976). "To each plutonic rock its proper name". Earth Science Reviews, V. 12: 1-33.

[24] Shapiro L, Brannock WW (1962). Rapid analysis of silicate, carbonate and phosphate rocks, U. S. Geol. Surv. Bull, 114 A: 56 p.

[25] Barker F (1979). Trondhjemite definition, environment and hypotheses of origin. In Barker (ed.): Trondhjemite, dacites and related rocks. Developments in Petrology, El Sevier Publishing Co., Amsterdam, V.6: 1-12.

[26] Irvine TN, Baragar WRA (1971). A guide to the chemical classification of the common volcanic rocks. Can. Jour. Earth Sci., 8: 523-548.

[27] Condie KC, Hunter DR (1976). Trace element geochemistry of Archean granitic rocks from the Barberton region, South Africa. Earth Planet. Sci. Let., 29: 389 - 400.

[28] Hunter DR (1979). The role of tonalitic and trondhjemitic rocks in the crustal development of Swaziland and the Eastern Transvaal, South Africa. In: Barker, F. (ed.): Trondhjemites, dacites and related rocks. Elsevier, Amsterdam: 303 - 322.

[29] Chappell BW, White AJR (1974). Two contrasting granite types: Pacific Geol., V.8: 284 -293.

[30] Middlemost EAK (1985). Magmas and magmatic rocks., Longman, London.

[31] Tuttle OF, Bowen NL (1958). Origin of granite in the light of experimental studies in the system $NaAlSi_3O_8$-$KAlSi_3O_8$-SiO_2- H_2O. Geol. Soc. Am. Em., 74: 153 p.

[32] Luth WC, Jams RH, Tuttle OF (1964). The granite system at pressure of 4 to 10 kilobars. J. Geophys. Res., V. 69: 759 -773.

[33] Hermes OD, Ballard RD, Banks PO (1978). Upper Ordovician peralkalic granites from the Gulf of Maine., Geol. Soc. Am. Bull. , v. 89:1761-1774.

[34] Maniar PD, Piccoli PM (1989). Tectonic discriminations of granitoids. Geol. Soc. Amer. Bull., 6: 129 - 198.

[35] Pearce JA, Harris NBW, Tindle AG (1984). Trace element discrimination diagrams for the tectonic interpretation of granitic rocks. J. Petrol., 25: 956 - 983.

[36] Gast PW (1965). Terrestrial ratio of potassium to rubidium and composition of the earth's mantle, Science, v.147: 858-860.

[37] Hart SR, Aldrich LT (1969). Fractionation of potassium/rubidium by amphiboles: Implications regarding mantle composition. Science, v.155: 325-327.

[38] Mason D (1966). Principals of geochemistry. 3rd (ed.),Wiley and Sons, New York: 310 p.

[39] Shaw DM (1968). A review of K/Rb fractionation trends by covariance analysis. Geochim. Cosmochim., Acta, V.32: 573-601.

[40] Taylor SR (1965). The application of trace element data to problems in petrology, in physical and chemistry of the Earth. Editors, Ahrens, L.H., Press, F, Runcor, S. K., and Urey, H. C.: 133 - 213.

[41] Cuney M, Leroy J, Volivezo A, Daziano C, Gambda B, Zarco AJ, Morello O, Ninci C, Molina P (1989). Metallogenesis of the uranium mineralized Achala granitic complex, Argentina: comparison with Hercynian peraluminous leucogranites of Western Europe. Proc. Tech. Comm. Meetings, Vienna, TECDOC-543, I.A.E.A., Vienna: 211 - 232.

[42] Meyer C, Hemley JJ (1967). Wall rock alterations, 166 – 235. Geochemistry of hydrothermal ore deposits (H. G. Barnes, ed.), Winston Inc. New York: 670 p.

[43] Nesbitt HW, Young GM (1984). Prediction of some weathering trends of plutonic and volcanic rocks based up on thermodynamic and kinetic consideration. Geochim. Cosmochim. Acta., 48: 1523 - 1534.

[44] Nesbitt HW, Young GM (1989). Formation and diagenesis of weathering profiles. J. Geol., 97: 129 - 147.

[45] Hasken LA, Haskin MA, Frey FA, Wildman TR (1968). Relative and absolute terrestrial abundance of the rare earths. In: Ahrens L. H. (ed.), Origin and distribution of the elements, vol. 1. Pergamon, Oxford: 889 - 911.

[46] Cullers RL, Graf L (1984). Rare earth elements in igneous rocks of the continental crust: intermediate and silicic rocks ore petrogenesis. In: Henderson, p. (ed.), Rare earth element geochemistry. El Sevier, Pub. Co., Amsterdam, V.2: 275-316.

[47] Grenne T, Roberts D (1998). The Holonda porphyrite, Norwegian Caledonides: geochemistry and tectonic setting of Early-Mid. Ordovician shoshonite volcanism. J. Geol. Soc., London, V.155: 131-142.

[48] Boyle RW (1982). Geochemical prospecting for thorium and uranium deposits. Develop. Economic, geol., 16, El Sevier, Amsterdam: 189 p.

[49] Hansink JP (1976). Equilibrium analysis of sandstone rollfront uranium deposits. Proceedings Inter. Symposium on exploration of uranium deposits. Int. Atomic Energy Agency, Vienna: 683 - 693.

[50] Stuckless JS, Nkomo IT, Winner DB, Van Trump G (1984). Geochemistry and uranium favourability of the postorogenic granites of the north-eastern Arabian Shield, Kingdom of Saudi Arabia, and Bull. Fac. Earth Sci., King Abdel Aziz Univ., No. 6: 195 - 209.